Size Comparison of Passive Devices of Buck-Boost-Type Converters With LC Filters in CCM: Theory and Method

Hugo R. Estofanero Larico *
Milton Evangelista de Oliveira Filho *
Valdir Pedrinho de Tomin Junior *
Roberto Santiago Alarcon Meza *

* *Technological Center of Joinville, Federal University of Santa Catarina, SC, (e-mail: hugo.larico@ufsc.br, milton.evangelista@ufsc.br, valdir.pedrinho@ufsc.br, roberto.s.a.m@posgrad.ufsc.br).*

Abstract:
This paper presents a comparison method of passive devices which is applied to buck-boost-type converters with LC filters in order to ascertain the topology for the compact design of such devices in continuous conduction mode (CCM). Design engineers can use the proposed method of size comparison to achieve an efficient and compact buck-boost converter, since volume of the passive devices generally defines converter size. Furthermore, this paper confirms that there is no an unique converter for any specifications instead of that there is a certain topology for a given specifications. This work considers the following buck-boost-type converters: the classical, the interleaved and the three-state switching cell topology. The three-state switching cell is included to show its greater capability to reduce the filter sizes, especially for design with duty cycles of around 1/2. This paper shows also that the filter arrangement is an option to reduce the volume of passive devices and, additionally to provide non-dissipative clamping of the switching devices. In this study idealized mathematical analysis was performed to compare the buck-boost-type converters.

Keywords: Buck-boost, interleaved, switching cell, filter, DC-DC converter.

1. INTRODUCTION

High-power density is a characteristic that is required in electronic converters in applications such as battery charger, electric vehicles, military and medical energy systems Lai et al. (2010), Fu et al. (2008),Heldwein and Kolar (2009),Raggl et al. (2009),Larico and Barbi (2013). However, research efforts are focused on the optimization of density of an unique converter. This study contributes to the research providing a size comparison of passive devices of a family of buck-boost-type converters with LC filters.

The buck-boost or non-isolated flyback converter shown in Fig. 1(a) is a classical dc-dc converter, which is widely used in applications where the step up/down characteristic is required Adib and Farzanehfard (2008), Ismail et al. (2008), Chen et al. (2013). However, this converter is the accumulative type, resulting in poor power density due to the large filter sizes Chen et al. (2006). Diverse techniques can be employed to reduce the filter sizes of buck-boost-type converters. A well-known technique is interleaving, which increases the current frequency across the input and output filters, reducing their sizes Xiao and Xie (2012),Blanes et al. (2013),Pavlovsky et al. (2014). On the other hand, this technique duplicates the number of inductors and semiconductor devices, as shown in Fig. 1(b), and these components operate at switching frequency and process half of load.

An other technique consists of substituting a single switching cell with a three-state switching cell (3SSC) Balestero et al. (2013, 2012); Araujo et al. (2010). The 3SSC buck-boost converter Balestero et al. (2013), shown in Fig. 1(c), increases the operation frequency at all filters, and only the autotransformer operates at switching frequency. Moreover, this technique provides theoretically zero current and zero voltage ripples across the filters for 50 % of the duty cycle.

Despite those characteristics, this study verify that combining the three-state switching cell with an alternative filter, an effective reduction in the total size of passive devices can be achieved. The three-state switching cell buck-boost converter with an alternative filter (AF-3SSC) Larico et al. (2020) is shown in Fig. 2.

This paper compares buck-boost-type converters with LC filters in continuous conduction mode (CCM). Initially, design equations of passive devices are developed using the AF-3SSC buck-boost converter. Afterwards, size comparison of the classical converter, the interleaved converter and the AF-3SSC converter is established.

2. AF-3SSC BUCK-BOOST CONVERTER: DESIGN EQUATIONS

In the classical buck-boost converter shown in Fig. 1(a), the input and output filters guarantee a continuous and

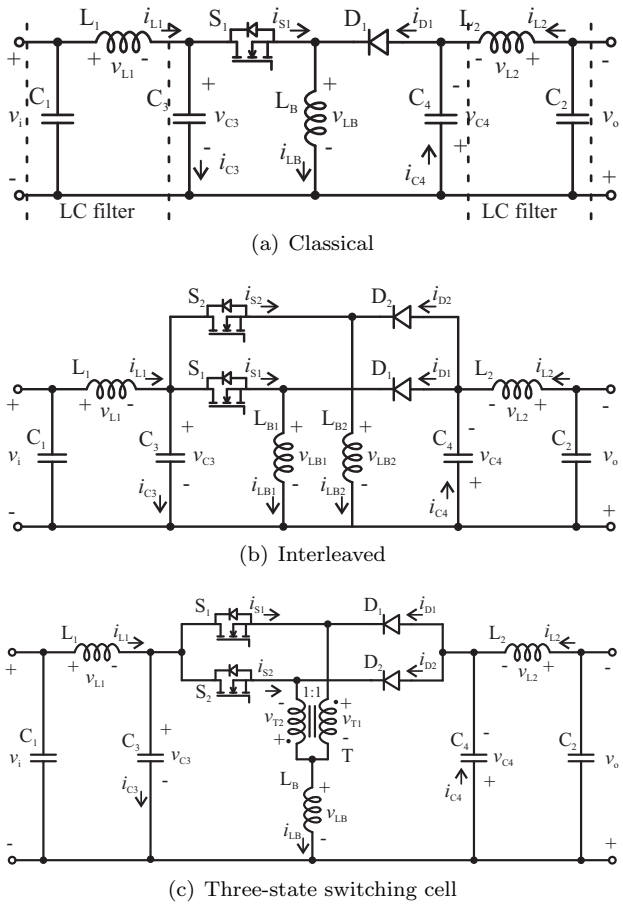

(a) Classical

(b) Interleaved

(c) Three-state switching cell

Figure 1. Buck-boost-type converters with LC filters.

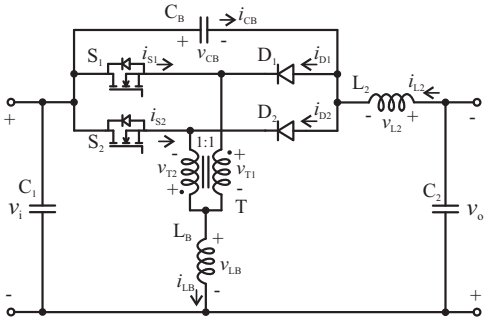

Figure 2. The alternative filter three-state switching cell buck-boost converter (AF-3SSC-BB converter).

constant current. However, in this configuration each filter operates independently, that is, those filters are designed to filter only the input or output current. Consequently, the total size of the converter increases considerably when low voltage ripples are required at both input and output source.

The AF-3SSC buck-boost converter proposed in Larico et al. (2020) and shown in Fig. 2 provides the following advantages:

- low current stresses across semiconductors;
- all filters operate in double switching frequency;
- the autotransformer operates in two quadrants of the BH curve, furthermore this device offers saturation immunity for small dc magnetic flux;
- the switching cell allows direct transfer of energy from source to load; and
- the alternative filter configuration improves the filter operation, allowing reduced number of components.

The main waveforms in non-overlapping and overlapping mode are shown in Figs. 4 and 5, respectively.

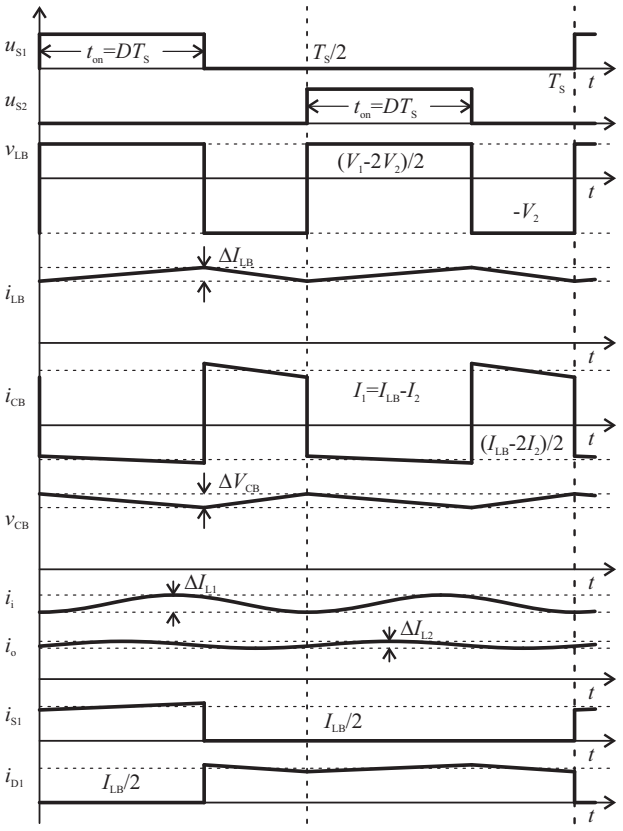

Figure 3. Main waveforms in non-overlapping mode in CCM.

2.1 Static characteristics in CCM

In this section the main equations in steady state are obtained. These equations are used to compute the capacitance and inductance of filters required in the AF-3SSC buck-boost converter.

Static gain All converters studied in this work have the same static gain that is given by

$$\frac{V_i}{V_o} = \frac{D}{1-D} \tag{1}$$

Current ripple across L_B Inductor L_B is the main storage device in classical topology, since this device processes all energy of the supplied to the load. However, in the AF-3SSC converter inductor L_B processes part of the energy supplied to the load. Consequently, there is a decrease in the current ripple across L_B as shown by the following equation:

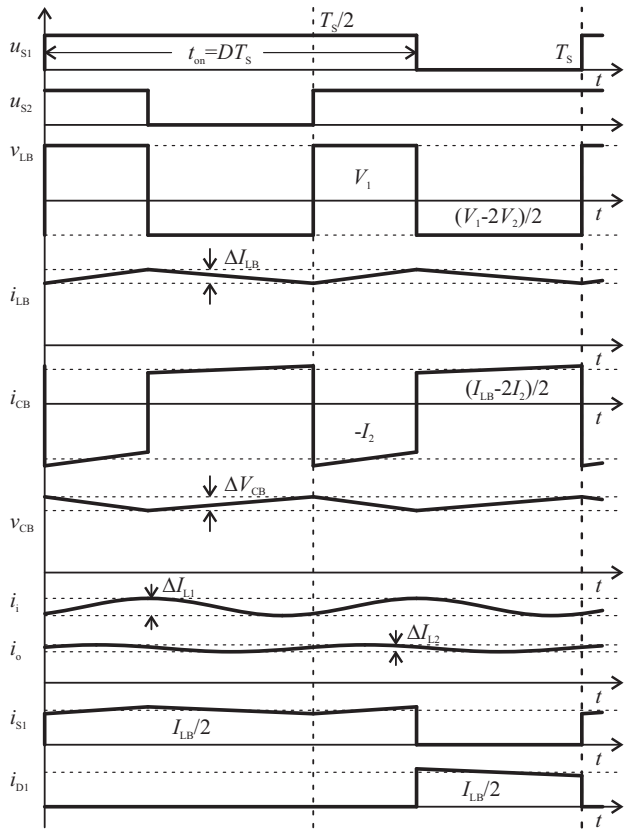

Figure 4. Main waveforms in overlapping mode in CCM.

$$\frac{\Delta I_{LB} L_B}{V_o T_s} = \begin{cases} \dfrac{1-2D}{2}, & \text{if} \quad D \leq 0.5 \\ \dfrac{(2D-1)(1-D)}{2D}, & \text{if} \quad D > 0.5 \end{cases} \tag{2}$$

Voltage ripple across C_B Capacitor C_B, as in the case of inductor L_B, processes part of the energy transfer to the load. Neglecting the current ripples introduced by inductors L_B and L_2, the capacitor current waveform becomes a rectangular current wave, the amplitude of which is defined by the average currents across the inductors. Thus, the voltage ripple across C_B can be computed by

$$\frac{\Delta V_{CB} C_B}{I_o T_s} = \begin{cases} \dfrac{(1-2D)D}{2(1-D)}, & \text{if} \quad D \leq 0.5 \\ \dfrac{(2D-1)}{2}, & \text{if} \quad D > 0.5 \end{cases} \tag{3}$$

Current ripple across L_2 Inductor L_2 filters the voltage ripple introduced by capacitor C_B. Neglecting the voltage ripple across capacitor C_2, the voltage applied to inductor L_2 is a triangular voltage wave, the respective current ripple of which is given by

$$\Delta I_{L2} = \frac{\Delta V_{CB}}{16 f_s L_2} \tag{4}$$

Voltage ripples across C_1 and C_2 Input and output capacitive filters guarantee low voltage ripple at the input and output sources. Capacitor C2 filters the current ripple introduced by inductor L2. Considering the voltage ripple across C1 and C2 to be smaller than the voltage ripple across CB, the fundamental component of Fourier's series of voltage wave across L2 is given by

$$V_{L2}{}^{2f_s} = \frac{\Delta V_{CB} |\sin(2D\pi)|}{2|1-2D| D\pi^2} \tag{5}$$

This component causes an alternating current across inductor L2 given by

$$I_{L2}{}^{2f_s} = \frac{\Delta V_{CB} |\sin(2D\pi)|}{8|1-2D| D\pi^3 f_s L_2} \tag{6}$$

Finally, the voltage ripple is given by

$$\Delta V_{C2} = \frac{\Delta V_{CB} |\sin(2D\pi)|}{16|1-2D| D\pi^4 f_s{}^2 L_2 C_2} \tag{7}$$

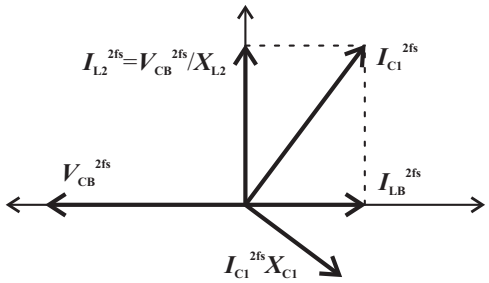

Figure 5. Phasor diagram used to compute ΔV_{C1}.

In the case of capacitor C1, the capacitor current is compounded by current ripples introduced by inductors L_B and L_2, as shown in Figs. 3 and 4. The total current across capacitor C1 is computed using the fundamental component of currents $\mathbf{I}_{LB}^{2fs}$ and $\mathbf{I}_{L2}^{2fs}$ as shown in Fig. 5. Therefore, the voltage ripple across C1 is given by

$$\Delta V_{C1} = \frac{1}{2\pi f_s C_1} \sqrt{\left(I_{LB}{}^{2f_s}\right)^2 + \left(I_{L2}{}^{2f_s}\right)^2} \tag{8}$$

where

$$I_{LB}{}^{2f_s} = \frac{\Delta I_{LB} |\sin(2D\pi)|}{2|1-2D| D\pi^2} \tag{9}$$

3. SIZE COMPARISON OF PASSIVE DEVICES: METHOD

The method consists of estimating and comparing the total size of capacitive and inductive devices, considering a unique design specification. The size comparison of the passive devices was carried out for the following conditions: filters operate at the same frequency, constant output voltage, input voltage varying within a certain range, PWM modulation, and continuous conduction mode.

3.1 Volume of magnetic and capacitive devices

For this purpose, the estimated volume equations given in Heldwein and Kolar (2009) are used, where the volume of a magnetic device is computed by

Table 1. Parameterized inductance and capacitance of the filters in the classical, the interleaved and the AF-3SSC buck-boost converters

Parameter	Value		
	Conventional	Interleaved	AF-3SSC
D		$D_{min} \leq D \leq D_{max}$	
f_s	$2\ f_s$	f_s	f_s
$\overline{L_B}$	$\frac{(1-D)^2}{2 \cdot \%\Delta I_{LB}}$	$\frac{2(1-D)^2}{\%\Delta I_{LB}}$	$\begin{cases} \frac{(1-2D)(1-D)}{2 \cdot \%\Delta I_{LB}}, & D \leq 0.5 \\ \frac{(2D-1)(1-D)^2}{2D \cdot \%\Delta I_{LB}}, & D > 0.5 \end{cases}$
$\overline{C_B}$	–	–	$\begin{cases} \frac{(1-2D)D^2}{2(1-D) \cdot \%\Delta V_{CB}}, & D \leq 0.5 \\ \frac{(2D-1)D}{2 \cdot \%\Delta V_{CB}}, & D > 0.5 \end{cases}$
$\overline{C_3}$	$\frac{D^2}{2(1-D) \cdot \%\Delta V_2}$	$\begin{cases} \frac{(1-2D)D^2}{2(1-D)^2 \cdot \%\Delta V_{C3}}, & D \leq 0.5 \\ \frac{(2D-1)D}{2(1-D) \cdot \%\Delta V_{C3}}, & D > 0.5 \end{cases}$	–
$\overline{C_4}$	$\frac{D}{2 \cdot \%\Delta V_2}$	$\begin{cases} \frac{(1-2D)D}{2(1-D) \cdot \%\Delta V_{C4}}, & D \leq 0.5 \\ \frac{(2D-1)}{2 \cdot \%\Delta V_{C4}}, & D > 0.5 \end{cases}$	–
$\overline{L_1}$	$\frac{(1-D)}{32 \cdot \%\Delta I_{L1}\overline{C_3}}$	$\begin{cases} \frac{(1-2D)}{32 \cdot \%\Delta I_{L1}\overline{C_3}}, & D \leq 0.5 \\ \frac{(1-D)(2D-1)}{32D \cdot \%\Delta I_{L1}\overline{C_3}}, & D > 0.5 \end{cases}$	–
$\overline{L_2}$	$\frac{D}{32 \cdot \%\Delta I_{L2}\overline{C_4}}$	$\begin{cases} \frac{(1-2D)D}{32(1-D) \cdot \%\Delta I_{L2}\overline{C_4}}, & D \leq 0.5 \\ \frac{(2D-1)}{32 \cdot \%\Delta I_{L2}\overline{C_4}}, & D > 0.5 \end{cases}$	$\begin{cases} \frac{(1-2D)D}{32(1-D) \cdot \%\Delta I_{L2}\overline{C_B}}, & D \leq 0.5 \\ \frac{(2D-1)}{32 \cdot \%\Delta I_{L2}\overline{C_B}}, & D > 0.5 \end{cases}$
$\overline{C_1}$	$\frac{D\sin(D\pi)/(1-D)^2}{16\pi^4 \cdot \%\Delta V_{C1} \cdot \overline{L_1} \cdot \overline{C_3}}$	$\frac{D\lvert\sin(2D\pi)\rvert/(1-D)^2}{32\pi^4 \cdot \%\Delta V_{C1} \cdot \overline{L_1} \cdot \overline{C_3}}$	$\frac{D\lvert\sin(2D\pi)\rvert}{8\pi^3(1-D)^2 \cdot \%\Delta V_{C1}} \cdots \cdot\sqrt{\left(\frac{1-D}{D\overline{L_B}}\right)^2 + \left(\frac{1}{4\pi\overline{L_2} \cdot \overline{C_B}}\right)^2}$
$\overline{C_2}$	$\frac{\sin(D\pi)/(1-D)}{16\pi^4 \cdot \%\Delta V_{C2} \cdot \overline{L_2} \cdot \overline{C_4}}$	$\frac{\lvert\sin(2D\pi)\rvert/(1-D)}{32\pi^4 \cdot \%\Delta V_{C2} \cdot \overline{L_2} \cdot \overline{C_4}}$	$\frac{\lvert\sin(2D\pi)\rvert/(1-D)}{32\pi^4 \cdot \%\Delta V_{C2} \cdot \overline{L_2} \cdot \overline{C_B}}$

$$Vol_{mag} = k_m(A_eA_w)^{\alpha_m} \tag{10}$$

where k_m and α_m are constants defined by a type of core. This equation shows that the volume of a magnetic device is a function of the product of the areas A_eA_w.

The area product of inductors can be approximately computed by

$$A_eA_w = \frac{LI_{Lmax}{}^2}{J_{max}B_{max}k_u} \tag{11}$$

The area product of an autotransformer is given by

$$A_eA_w = \frac{V_2I_{LBmax}}{2f_sJ_{max}B_{max}k_u} \tag{12}$$

The volume of a film capacitor is directly proportional to the maximum capacitor charge Heldwein and Kolar (2009).

$$Vol_{cap} = k_{cap}Q_{Cmax} = k_{cap}CV_{Cmax} \tag{13}$$

3.2 Percentage of current and voltage ripples

These quantities are defined as the rate of current or voltage ripple to respective average value as shown as follow:

$$\begin{aligned} \%\Delta I &= \frac{\Delta I}{I} \\ \%\Delta V &= \frac{\Delta V}{V} \end{aligned} \tag{14}$$

The percentage values allow a comparison between the buck-boost-type converters, since they reflect the perfor-

mance of the filter devices. On the other hand, the percent current ripple of inductor L_B provides information of the minimum power load that the converter can operate within continuous conduction mode.

3.3 Parameterized quantities

The parameterization of the quantities is employed to avoid using the values of some parameters. In this study the switching frequency, output current and output voltage are used as base parameters and, therefore the parameterized inductance and capacitance are defined as

$$\overline{L} = \frac{I_o L}{T_s V_o} \tag{15}$$

$$\overline{C} = \frac{V_o C}{T_s I_o} \tag{16}$$

Using the definitions established by equations (14)-(16), the parameterized inductances and capacitances listed in Table 1 are obtained, corresponding to the classical, the interleaved and the AF-3SSC buck-boost converters in CCM. The comparison requires that the operation frequency of input and output filters should be the same to all converters for that reason, the classical converter is operated with twice switching frequency. It can be noted that parametrized quantities of the input and output filters require computing of parametrized values of L_B, C_B, C_3 and C_4.

The parametrized inductances and capacitances show in Table 1 allow to find the critical inductances and capacitances which guarantee the ripple requirements in filters.

3.4 Total parameterized volume of passive devices

The capacitor parameterized volume is defined as

$$\overline{Vol_{cap}} = \frac{Vol_{cap}}{k_{cap} I_2 T_s} \tag{17}$$

The total size of the capacitors for the converters studied is given by

$$\overline{Vol_{cap_T}} = (\overline{C_1} + \overline{C_3} + \overline{C_B})\frac{(1-D)}{D} + \overline{C_2} + \overline{C_4} + \overline{C_B} \tag{18}$$

The parameterized volume of the magnetic devices is defined as

$$\overline{Vol_{mag}} = \left(\overline{A_e A_w}\right)^{\alpha_m} \tag{19}$$

where

$$\overline{Vol_{mag}} = \frac{Vol_{mag}}{k_m}\left(\frac{k_u J_{max} B_{max}}{T_s P_2}\right)^{\alpha_m}$$

$$\overline{A_e A_w} = \frac{A_e A_w k_u J_{max} B_{max}}{T_s P_2}$$

Applying these equations to each one of the buck-boost-type converters, the total magnetic parameterized volume result in:

$$\overline{Vol_{mag_T}} =$$

- Classical converter

$$\left(\frac{\overline{L_B}}{(1-D)^2}\right)^{\alpha_m} + \left(\frac{\overline{L_1} D^2}{(1-D)^2}\right)^{\alpha_m} + \left(\overline{L_2}\right)^{\alpha_m} \tag{20}$$

- Interleaved converter

$$2\left(\frac{\overline{L_B}}{4(1-D)^2}\right)^{\alpha_m} + \left(\frac{\overline{L_1} D^2}{(1-D)^2}\right)^{\alpha_m} + \left(\overline{L_2}\right)^{\alpha_m} \tag{21}$$

- AF-3SSC converter

$$\left(\frac{\overline{L_B}}{(1-D)^2}\right)^{\alpha_m} + \left(\overline{L_2}\right)^{\alpha_m} + \left(\frac{1}{2(1-D)}\right)^{\alpha_m} \tag{22}$$

Equations (18) and (20)-(22) allow computing the total parametrized volume of capacitive and magnetic devices, respectively. The parametrized capacitances and inductances in equations represent the critical capacitances and inductances which guarantee the requirements of voltage and current ripples. The duty cycle in equations arises due to the base of the parametrization, for example, in (18) charges in C1 and C3 depend on input voltage that can be expressed as a function of the output voltage and the duty cycle. In (22) the last component represents the parametrized volume of the transformer of the three state switching cell.

Table 2. Comparison of the buck-boost-type converters: dimensionless quantities

Parameter	Value		
	Conventional	Interleaved	AF-3SSC
V_o	V_o		
D	$0.4 \leq D \leq 0.6$		
V_i	$1.5V_o \geq V_i \geq 0.667V_o$		
f_s	2 f_s	f_s	f_s
$\overline{C_B}$	–	–	0.6
$\overline{C_3}$	4.50	1.5	–
$\overline{C_4}$	3	1	–
$\overline{C_1}$	1.743	1.616	2.145
$\overline{C_2}$	1.017	0.942	0.942
$\overline{Vol_{cap_T}}$	13.38	6.61	5.66
$\overline{L_B}$	1.8	7.2	0.6
$\overline{L_1}$	0.0417	0.0417	–
$\overline{L_2}$	0.0625	0.0625	0.104
$\overline{Vol_{mag_T}}$	5.83	11.34	3.91

3.5 Numerical analysis

Figure 6 shows the total parameterized size of the capacitive (a) and magnetic (b) devices. The curves shown the total volume for different duty cycle ranges from 20 %, 30 %, 40 % and 50 % to any high value, and using the following specifications:

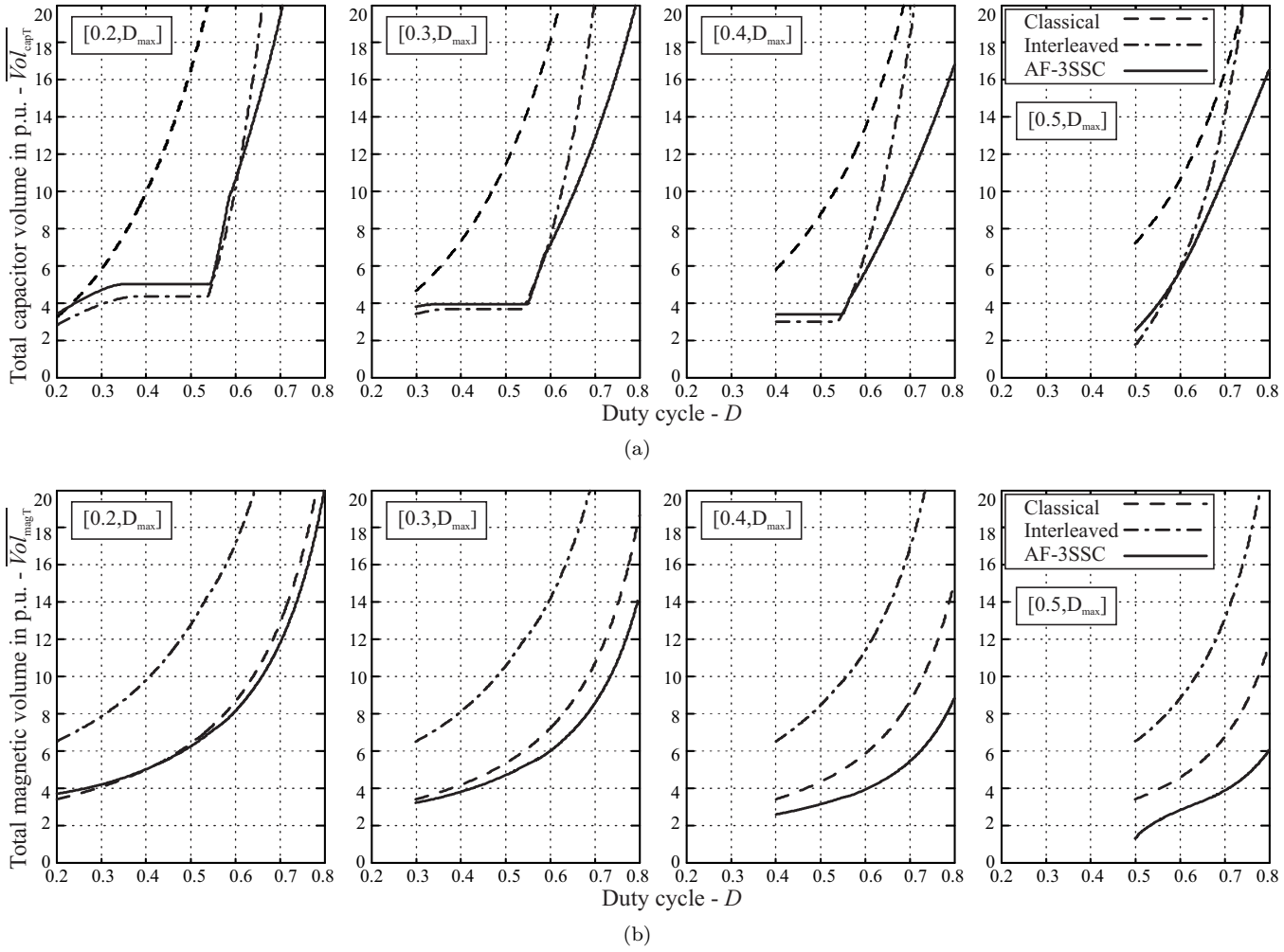

Figure 6. Parameterized total of the passive devices: (a) capacitors and (b) magnetic devices.

$$\begin{aligned} &\%\Delta I_{LB} \leq 10\ \%; \\ &\%\Delta I_{L1} = \%\Delta I_{L2} \leq 10\ \%; \\ &\%\Delta V_{CB} = \%\Delta V_{C3} = \%\Delta V_{C4} \leq 10\ \%; \\ &\%\Delta V_{C1} \leq 0.7\ \% \text{ and} \\ &\%\Delta V_{C2} \leq 0.8\ \% \end{aligned} \tag{23}$$

The total size of the magnetic devices was computed using $\alpha = 0.705$ into (15)-(22). The parameterized inductance and capacitance required by the filters are obtained using the equations given in Table 1. These parameters represent the minimum values required to adhere to the current and voltage ripple specifications.

The comparison shows that the AF-3SSC converter provides a compact design of passive device, when the design requires operation in a wide range of duty cycles. In addition, the curves for the magnetic volume show that the AF-3SSC converter provides magnetic devices with a small total size for all design ranges from 30 % of duty cycle. On the other hand, the curves also show with the interleaved converter a high total size is obtained for the magnetic devices, but a low total size is obtained for the capacitive devices for operation in a small range of duty cycle.

Table 2 shows parameterized volume of each passive device and the total volume for a duty cycle range of 40 % to 60 %. On establishing the total sizes for the classical converter as a reference for comparison, the capacitor and magnetic total sizes for the AF-3SSC converter represents 42.3 % and 67 %, respectively, while the corresponding values for the interleaved converter are 49.4 % and 194.5 %.

These results show that for specification given in (23) and Table 2, the AF-3SSC converter has a better performance in terms of the total size of passive devices. Moreover, the results show that the interleaved buck-boost converter is able to reduce the capacitor total size, but this converter increases considerably the total size of the magnetic devices.

4. 3D CAD SIZE COMPARISON

The information given in Table 2 was used to specify the passive devices of a 200 W converter based on the classical, the interleaved and the AF-3SSC buck-boost converters. The components required for each design are shown in Table 3. The capacitors and magnetic cores listed in Table 3 are common types produced by the same manufacturer. The magnetic devices were designed considering $J_{max} = 400$ A/cm^2, $B_{max} = 0.3$ T and $k_u = 0.5$.

The comparison based on Table 3 shows that the total sizes of the capacitor and magnetic devices for the 3SCC

Table 3. Comparison of the buck-boost converters: physical quantities

Param.	Classical			Interleaved			AF-3SSC		
P_o/V_o	200 W/48 V								
D	$0.4 \leq D \leq 0.6$								
V_i	72 V$\geq V_i \geq$ 32 V								
f_s	90 kHz			45 kHz			45 kHz		
Cap.	Computed (μF)	Selected (μF)	Volume (cm^3)	Computed (μF)	Selected (μF)	Volume (cm^3)	Computed (μF)	Selected (μF)	Volume (cm^3)
C_B							1.15	2x0.68 (160 V)	2x1.36
C_1	3.36	1x3.3 (100 V)	1x3.82	3.11	1x3.3 (100 V)	1x3.82	4.13	2x2.2 (100 V)	2x2.88
C_3	8.68	4x2.2 (100 V)	4x2.88	2.89	3x1 (100 V)	3x1.82			
C_2	1.96	2x1 (63 V)	2x0.99	1.81	2x1 (63 V)	2x0.99	1.81	2x1 (63 V)	2x0.99
C_4	5.78	1x4.7 (63 V)	1x3.82	1.92	2x1 (63 V)	2x0.99			
		1x1 (63 V)	1x0.99						
Vol_{cap}			22.1			13.2			10.4
Mag./ A_eA_w	Computed (μH)/ (cm^4)	Selected (core)/ (cm^4)	Volume (cm^3)	Computed (μH)/ (cm^4)	Selected (core)/ (cm^4)	Volume (cm^3)	Computed (μH)/ (cm^4)	Selected (core)/ (cm^4)	Volume (cm^3)
L_B/	460.8	E 55/28/21	126.29	2x1800	2xE 55/28/21	2x126.29	153.6	E 42/21/15	58.41
A_eA_w	8.33	8.85		2x8.33	2x8.85				
L_1/	10.6	E 20/10/5	5.26	10.6	E 20/10/5	5.26			
A_eA_w	0.069	0.08		0.069	0.08				
L_2/	16	E 20/10/5	5.26	16	E 20/10/5	5.26	26.6	E 20/10/5	5.26
A_eA_w	0.046	0.08		0.046	0.08		0.077	0.08	
T/							T	E 30/15/14	26.01
A_eA_w							0.925	1.02	
Vol_{mag}			136.8			263.1			89.4

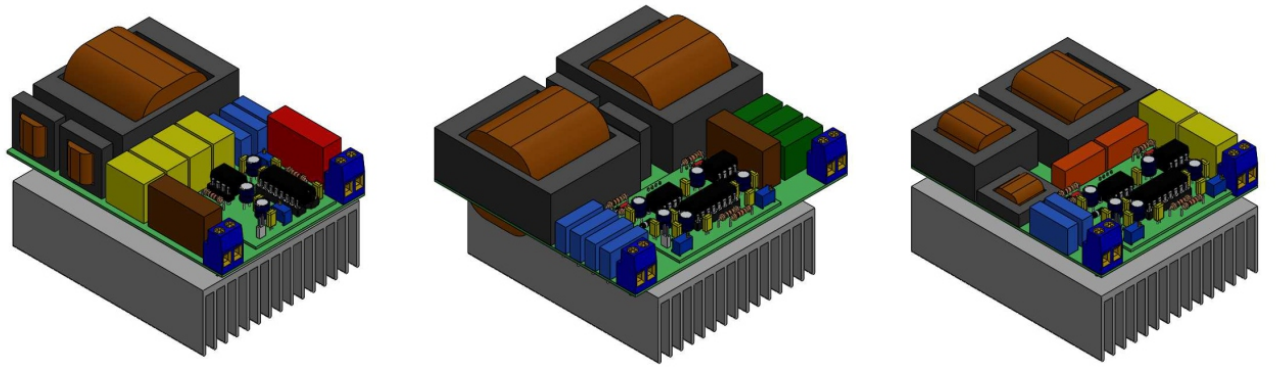

(a) Classical: 74x102x63mm/475.5cm^3 (b) Interleaved: 100x95x63mm/598.5cm^3 (c) AF-3SSC: 74x90x55mm/366.3cm^3

Figure 7. Size comparison of 3D CAD drawing of buck-boost-type converters with LC filters.

converter represent 47 % and 65.3 %, respectively, of those required in the classical converter. In the interleaved version, the filter sizes represent 59.7 % and 192.3 %, respectively. It can be noted that these results are close to the theoretically values reported in the previous section. This confirms the good performance of the comparison method which was established to obtain a compact buck-boost-type converter.

Figure 7 shows size comparison of 3D CAD drawing of the classical, the interleaved and the AF-3SSC buck-boost converter. Converter size of the AF-3SSC represent 77 % of size of the classical converter, while size of the interleaved converter represent 126 %.

5. CONCLUSIONS

In this paper a size comparison method of passive devices of buck-boost-type converters with LC filters has been presented. This work considers the following buck-boost-type converters: the classical, the interleaved and the three-state switching cell topology. The three-state switching cell buck-boost converter with a compact filter (AF-3SSC

buck-boost converter) was employed to get design equations in continuous conduction mode.

The comparison method was established considering a certain range of duty cycles and a given specifications where the AF-3SSC converter provides a better performance of size. The results from the theoretical comparison method were closed to the size trend of passive devices in a 200 W prototype design. In both cases the AF-3SSC converter provided passive devices with small total size. On the other hand, the interleaved converter increased considerably the total size for studied cases, therefore the interleaved converter should be avoided when a compact converter is required in such conditions.

Moreover, size comparison of the 3D CAD drawing showed that size of the AF-3SSC converter represented 77 % of size of the classical converter, while size of the interleaved converter represented 126 %. It can be noted that these results followed the trend of total pamametrized size of the magnetic devices.

Furthermore, in this case a good efficiency is expected since a reduction in size of the passive devices decreases the conduction losses, while the intrinsic clamped circuit (capacitor C_B) recoveries part of the turn off switching energy losses, reducing the switching losses.

Finally, the researchers and design engineers can be extended the proposed method of size comparison to achieve a compact converter from a family of same-type converters in continuous conduction mode for a given specifications. This paper shows also that the filter configuration can be an option to reduce the total size of passive devices.

REFERENCES

Adib, E. and Farzanehfard, H. (2008). Family of zero-current transition pwm converters. *Industrial Electronics, IEEE Transactions on*, 55(8), 3055–3063. doi:10.1109/TIE.2008.922597.

Araujo, S., Torrico-Bascope, R., and Torrico-Bascope, G. (2010). Highly efficient high step-up converter for fuel-cell power processing based on three-state commutation cell. *Industrial Electronics, IEEE Transactions on*, 57(6), 1987–1997. doi:10.1109/TIE.2009.2029521.

Balestero, J., Tofoli, F., Fernandes, R., Torrico-Bascope, G., and de Seixas, F. (2012). Power factor correction boost converter based on the three-state switching cell. *Industrial Electronics, IEEE Transactions on*, 59(3), 1565–1577. doi:10.1109/TIE.2011.2160136.

Balestero, J., Tofoli, F., Torrico-Bascope, G., and de Seixas, F. (2013). A dc-dc converter based on the three-state switching cell for high current and voltage step-down applications. *Power Electronics, IEEE Transactions on*, 28(1), 398–407. doi:10.1109/TPEL.2012.2197419.

Blanes, J., Gutierrez, R., Garrigos, A., Lizan, J., and Cuadrado, J. (2013). Electric vehicle battery life extension using ultracapacitors and an fpga controlled interleaved buck-boost converter. *Power Electronics, IEEE Transactions on*, 28(12), 5940–5948. doi:10.1109/TPEL.2013.2255316.

Chen, J.J., Shen, P.N., and Hwang, Y.S. (2013). A high-efficiency positive buck-boost converter with mode-select circuit and feed-forward techniques. *Power Electronics, IEEE Transactions on*, 28(9), 4240–4247.

Chen, J., Maksimovic, D., and Erickson, R. (2006). Analysis and design of a low-stress buck-boost converter in universal-input pfc applications. *Power Electronics, IEEE Transactions on*, 21(2), 320–329. doi:10.1109/TPEL.2005.869744.

Fu, D., Lee, F., Qiu, Y., and Wang, F. (2008). A novel high-power-density three-level lcc resonant converter with constant-power-factor-control for charging applications. *Power Electronics, IEEE Transactions on*, 23(5), 2411–2420. doi:10.1109/TPEL.2008.2002052.

Heldwein, M. and Kolar, J. (2009). Impact of emc filters on the power density of modern three-phase pwm converters. *Power Electronics, IEEE Transactions on*, 24(6), 1577–1588. doi:10.1109/TPEL.2009.2014238.

Ismail, E., Sabzali, A., and Al-Saffar, M. (2008). Buck-boost-type unity power factor rectifier with extended voltage conversion ratio. *Industrial Electronics, IEEE Transactions on*, 55(3), 1123–1132.

Lai, R., Wang, F., Ning, P., Zhang, D., Jiang, D., Burgos, R., Boroyevich, D., Karimi, K., and Immanuel, V. (2010). A high-power-density converter. *Industrial Electronics Magazine, IEEE*, 4(4), 4–12. doi:10.1109/MIE.2010.938722.

Larico, H.R.E. and Barbi, I. (2013). Three-phase flyback push-pull dc-dc converter: Analysis, design, and experimentation. *Power Electronics, IEEE Transactions on*, 28(4), 1961–1970. doi:10.1109/TPEL.2012.2211037.

Larico, H.R.E., de Tomin, V.P., and Larico, E.R.E. (2020). Unified second-stage lc filter applied in the three-state switching cell buck–boost converter: Static and dynamic analysis and experimentation. *IEEE Transactions on Industrial Electronics*, 67(1), 225–234. doi:10.1109/TIE.2019.2892674.

Pavlovsky, M., Guidi, G., and Kawamura, A. (2014). Assessment of coupled and independent phase designs of interleaved multiphase buck/boost dc-dc converter for ev power train. *Power Electronics, IEEE Transactions on*, 29(6), 2693–2704. doi:10.1109/TPEL.2013.2273976.

Raggl, K., Nussbaumer, T., Doerig, G., Biela, J., and Kolar, J. (2009). Comprehensive design and optimization of a high-power-density single-phase boost pfc. *Industrial Electronics, IEEE Transactions on*, 56(7), 2574–2587. doi:10.1109/TIE.2009.2020074.

Xiao, H. and Xie, S. (2012). Interleaving double-switch buck-boost converter. *Power Electronics, IET*, 5(6), 899–908. doi:10.1049/iet-pel.2011.0166.